Electronic Supporting Information

Two-dimensional $NiCo_2O_4$ nanosheet-coated three-dimensional graphene networks for high-rate, long-cycle-life supercapacitors

Jiang Zhou[a,b], *Ying Huang*[a], *Xiehong Cao*[a], *Bo Ouyang*[a], *Wenping Sun*[a], *Chaoliang Tan*[a], *Yu Zhang*[a], *Qinglang Ma*[a], *Shuquan Liang*[b*], *Qingyu Yan*[a], *and Hua Zhang*[a*]

[a]School of Materials Science and Engineering, Nanyang Technological University, 50 Nanyang Avenue, Singapore, 639798, Singapore. E-mail: hzhang@ntu.edu.sg. Website: http://www.ntu.edu.sg/home/hzhang/.

[b]School of Materials Science and Engineering, Central South University, Changsha, 410083, China.E-mail:lsq@mail.csu.edu.cn

Experimental section.

Chemicals: All chemicals used in our experiments are of analytical purity and used as received without further purification. Nickel (II) chloride hexahydrate ($NiCl_2 \cdot 6H_2O$), cobal (II) chloride hexahydrate ($CoCl_2 \cdot 6H_2O$), urea ($CO(NH_2)_2$) were purchased from Sigma-Aldrich. Ethanol, methanol and acetone were were purchased from Fisher chemical. Nickel foams were purchased from Changsha lyrun new material Co. Ltd (China). Milli-Q water (18.2MΩ cm, Milli-Q System, Millipore, USA) were used in all experiments.

Synthesis of three-dimensional graphene network on Nickel foam (3DGN) by CVD: The preparation of 3DGN was based on our previous work with slight modification.[1-3] In a typical experiment, nickel foams were placed in a quartz tube furnace and heated to 1000 °C at a heating rate of ~37 °C min^{-1} in the flow of mixed gas of Ar (160 sccm) and H_2 (40 sccm). The temperature was kept at 1000 °C for 10 min and then naturally cooled down to 900 °C. After the temperature of furnace was stable at 900 °C, ethanol was bubbled into the tube with the H_2 flow (20 sccm) and the Ar flow (80 sccm) for 15 min. Then the furnace was fast cooled down to room temperature under the protection of Ar and H_2 at a cooling rate of ~100 °C min^{-1}.

Synthesis of $NiCo_2O_4$ nanosheets on 3DGN ($NiCo_2O_4$ NS/3DGN): Typically, 0.2 mmol $NiCl_2 \cdot 6H_2O$ and 0.4 mmol $CoCl_2 \cdot 6H_2O$ were added into a mixture of 5 ml of Milli-Q water and 30 mlof methanolwith vigorously magnetic stirring at room temperature and then 30 mmol of urea was added into the aforementioned mixture. After 15 min, the above solution was transferred into a autoclave liner. A piece of 3DGN was wrapped by Teflon tape with exposure area of 1cm^{-2} was immersed into the reaction solution. The liner was sealed in a stainless steel autoclave and kept in an electrical oven at 120 ^oC for 6 h. After cooling down naturally, the obatined NiCo-precursor/3DGN was taken out from the autoclave liner and washed with Milli-Q water and anhydrous ethanol several times, followed by drying at 60 ^oC overnight. The $NiCo_2O_4$ NS/3DGN were obtained by calcining the NiCo-precursor/3DGN in air at 300^oC for 2 h with a heating ramp rate of 1^oC min^{-1}.

Characterization: The prepared samples were characterized by X-ray diffractometer (XRD-600, Shimadzu, Japan) using Cu Kα radiation (λ=1.54178 Å) and X-Ray photoelectron spectroscopy (XPS, Kratos-Axis Ultra System) with monochromatized Al-Kα radiation. Raman spectra were collected with a WITEC CRM200 Raman System (488 nm laser, 2.54 eV, WITec, Germany). The SEM images were taken with a field emission scanning electron microscopy (FESEM, Model JSM-7600F, JEOL Ltd., Tokyo, Japan). Transmission electron microscopy (TEM) and selected-area electron diffraction (SAED) images were obtained on a transmission electron microscopy (TEM, JEM-2100F, JEOL Ltd., Tokyo) with energy dispersive X-ray spectroscopy (EDX). The thickness of samples was characterized by atomic force microscopy (AFM, Dimension 3100 Veeco, CA, USA). Prior to AFM measurement, the sample was first sonicated in Milli-Q water for about 10 min, and then a drop of the solution was dropped on a silicon substrate and dried naturally.

Electrochemical measurements: Cyclic voltammetry (CV) and galvanostatic charge-discharge performances were measured using a standard three-electrode testing system in the electrolyte of 6 M KOH aqueous solution and recorded on Solartron analytical equipment (Model 1470E, AMETEK, UK). The prepared $NiCo_2O_4$ NS/3DGN was directly used as the working electrode. A Pt wire and Ag/AgCl electrode (saturated KCl) were used as the counter electrode and reference electrode, respectively. The specific capacitance and current density were calculated based on the weight of active materials. The mass loading of active materials on 3DGN for electrochemical test is around 0.7 mg after calcination. The nominal area of $NiCo_2O_4$ NS/3DGN electrode immersed into the electrolyte was controlled to be around 1 cm×1 cm. The specific capacitance was obtained from the equation,[4, 5]

$$C = \frac{I \times \Delta t}{m \times \Delta V}$$

Where C (F/g) is the specific capacitance, I (mA) is the discharge current, Δt (s) is the discharge time, ΔV (V) is the potential drop during discharge process after internal resistance (IR) drop, and m (g) is the mass of active materials only.

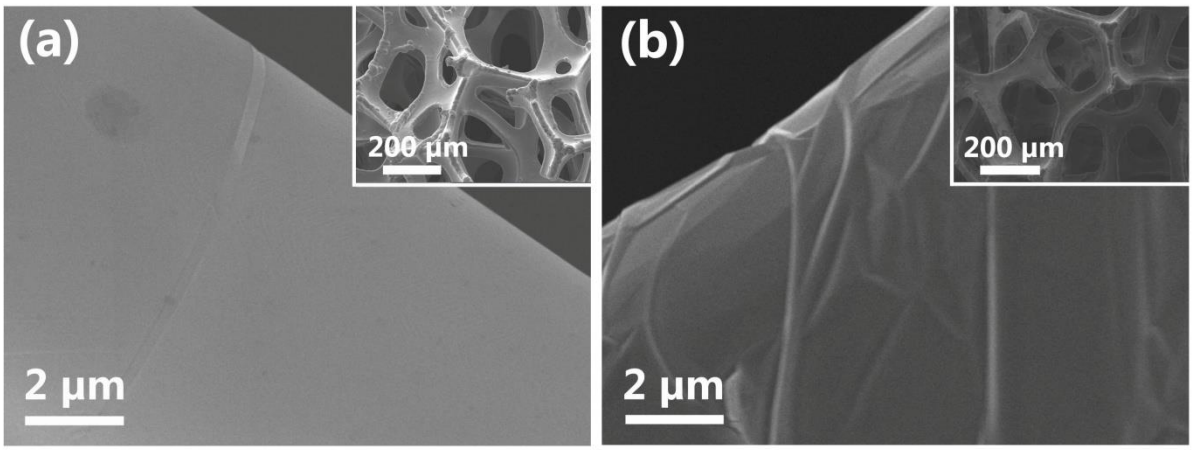

Figure S1. SEM images of (a) pure Ni foam and (b) 3DGN on Ni foam. Insets: The corresponding low-magnification SEM images.

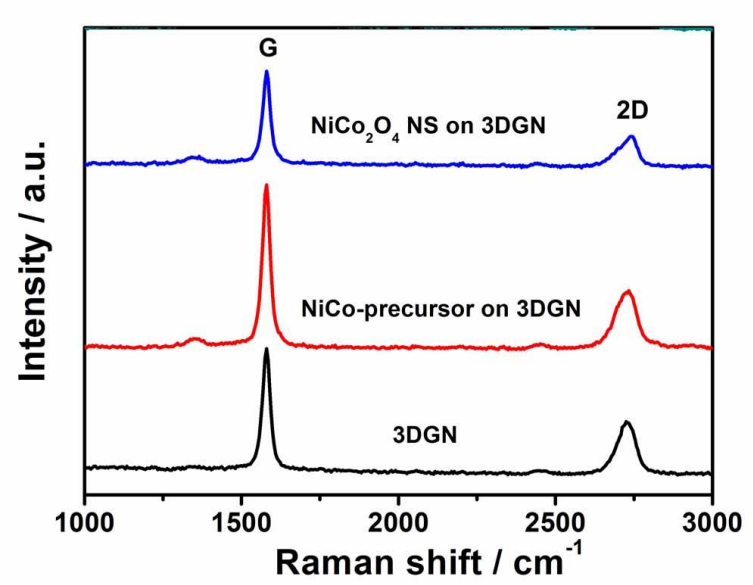

Figure S2. Raman spectra of 3DGN, NiCo-precursor/3DGN, and $NiCo_2O_4$ NS/3DGN.

Figure S3. Photos of $NiCo_2O_4$ NS/3DGN electrode with different bending angles: (a) as-prepared, (b) bent at ~45°, (c) bent at ~90°, and (d) recovered.

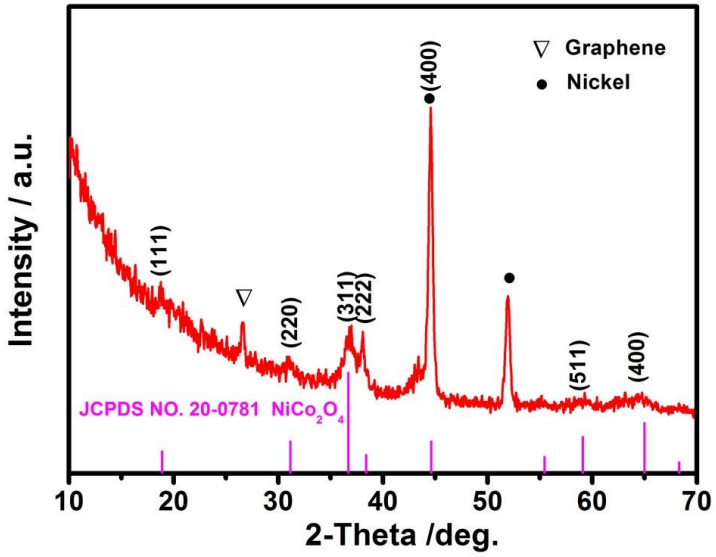

Figure S4. XRD patterns of $NiCo_2O_4$ NS/3DGN.

To prepare sample for XRD, the $NiCo_2O_4$ NS/3DGN hybrid was first sonicated in ethanol for about 5 h. Then the solution was dropped on glass. After drying, it was used for XRD characterization. As shown in Figure S4, well-defined diffraction peaks of (111), (220), (311), (222), (400), (511) and (400) are clearly observed, which can be ascribed to the spinel $NiCo_2O_4$ crystalline structure [space group: *F*3 (020)*, JCPDF Card No. 20-0781], with the standard peaks depicted by the pink lines. This result is consistent with those in previous reports.[6-8] The diffraction peak at $2\theta=26.5^o$ can be attributed to graphitic carbon.[9,10] Moreover, two characteristic peaks located at $2\theta=44.5^o$ and 51.8^o in the XRD patterns arise from the Ni foam substrate (JCPDS Card No. 65-2865), which are also reported in the 3D graphene grown

on Ni foam.[11,12] The XRD result indicates that the $NiCo_2O_4$ NS/3DGN hybrid has been successfully prepared by the solvothermal reaction and then calcination at 300°C.

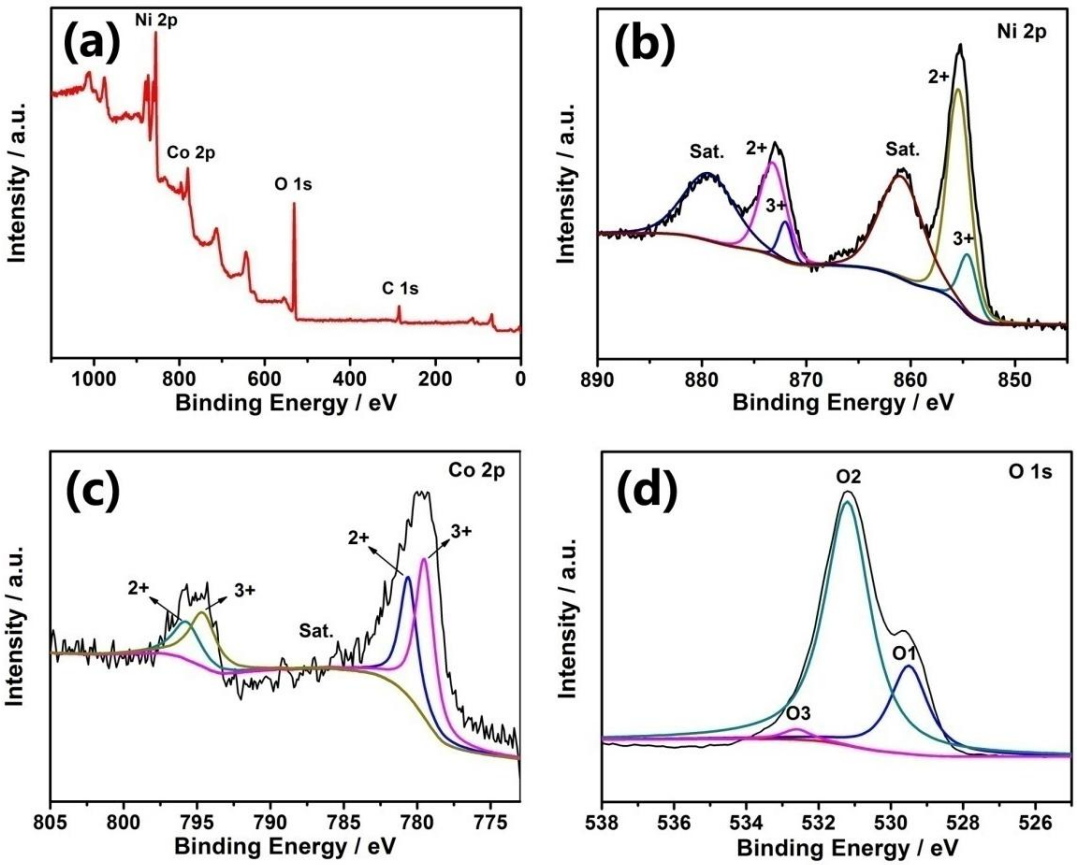

Figure S5. XPS spectra of $NiCo_2O_4$ NS/3DGN: (a) survey spectrum, (b) Ni 2p core level, (c) Co 2p core level, and (d) O 1s core level.

To prepare samples for XPS, the $NiCo_2O_4$ NS/3DGN hybrid was first sonicated in ethanol for about 2 h. Then the solution was dropped on silicon substrate. After drying, it was used for XPS characterization. To obtain further evidence for the chemical bonding state and composition of the $NiCo_2O_4$ NS/3DGN, X-Ray photoelectron spectroscopy (XPS) was performed and the spectra are shown in Figure S5. Typical signals of Ni 2p, Co 2p, O 1s core levels were detected based on the survey spectrum (Figure S5a), which are consistent with previous reports.[8,13,14] The Ni 2p spectra, as presented in Figure S5b, can be fitted with two spin-orbit doublets characteristic of $Ni^{2+}$and Ni^{3+} and two shakeup satellites. Specifically, the

fitting peaks at 855.5 and 873.3 eV are ascribed to Ni^{2+}, while the peaks at 854.6 and 872 eV are assigned to Ni^{3+}.[13] In the Co 2p spectra (Figure S5c), two kinds of Co species ($Co^{2+}$and Co^{3+}) are detected. The fitting peaks at 780.6 and 795.8 eV are ascribed to Co^{2+}, while the peaks at 779.5 and 794.7 eV are ascribed to Co^{3+}.[13,15] The O 1s spectra (Figure S5d) show three contributions, denoted as O1(529.5 eV), O2 (531.2 eV), and O3 (532.6 eV), associated with typical metal-oxygen bonds, the high number of defect sites with low oxygen coordination in the material with small particle size, and the multiplicity of physic/chemisorbed water on and within the surface, respectively.[14,16-18]

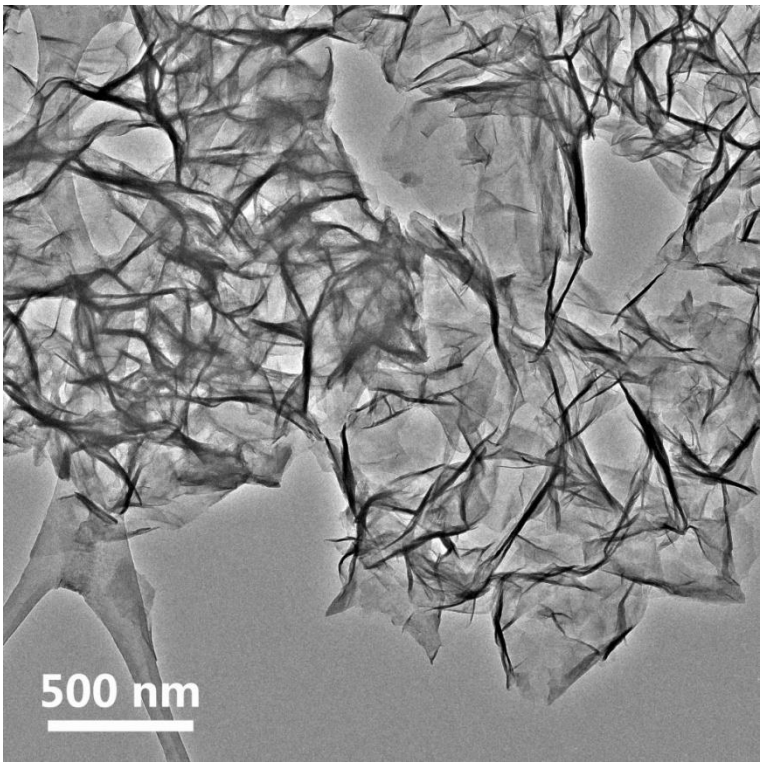

Figure S6. TEM image of NiCo-precursor/3DGN.

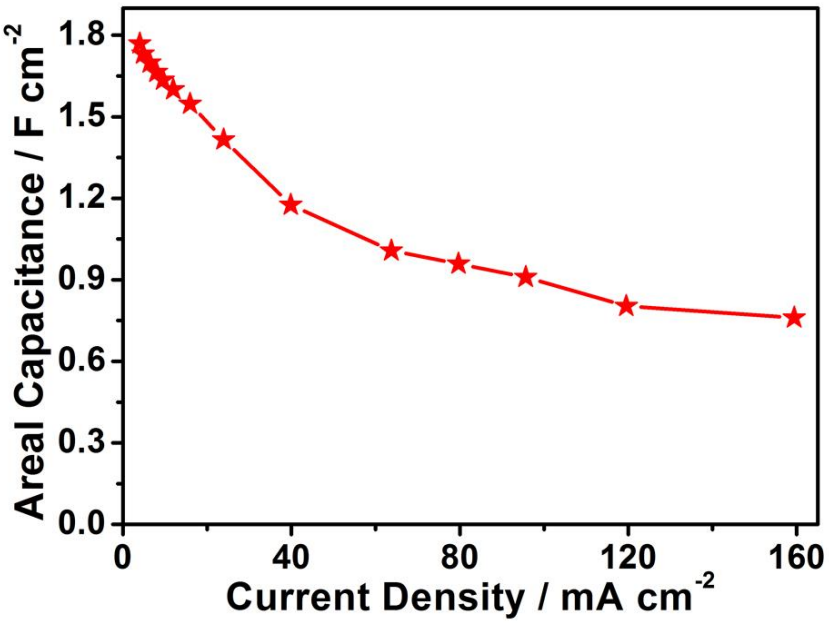

Figure S7. The areal capacitance of $NiCo_2O_4$ NS/3DGN electrode as a function of current density.

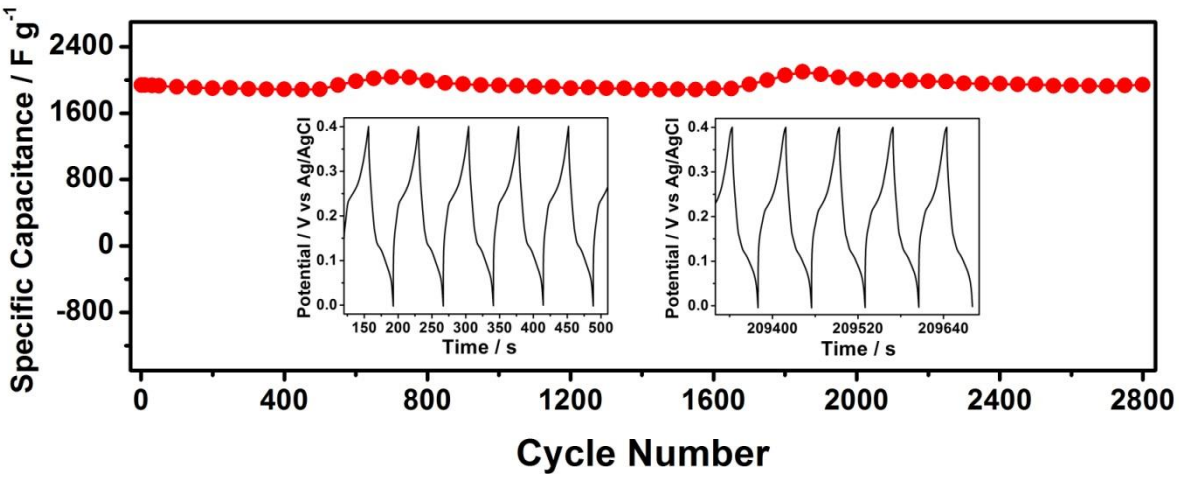

Figure S8. Cycling stability of $NiCo_2O_4$ NS/3DGN electrode at the current density of 20 A g^{-1}. Insets: The first and the last 5 charge/discharg curves for the electrode. The potential range is from 0 to 0.4 V (vs. standard Ag/AgCl electrode).

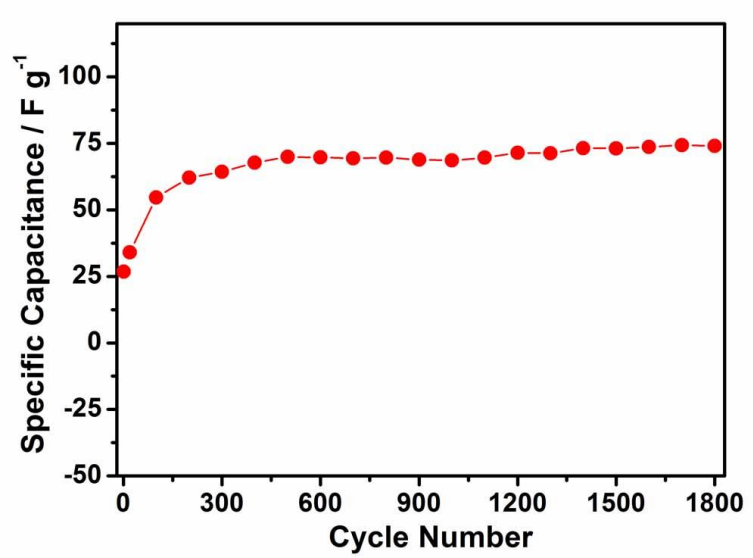

Figure S9. Cycling performance of pure 3DGN electrode at the current density of 2 A g^{-1}. The potential range is from 0 to 0.4 V (vs. standard Ag/AgCl electrode).

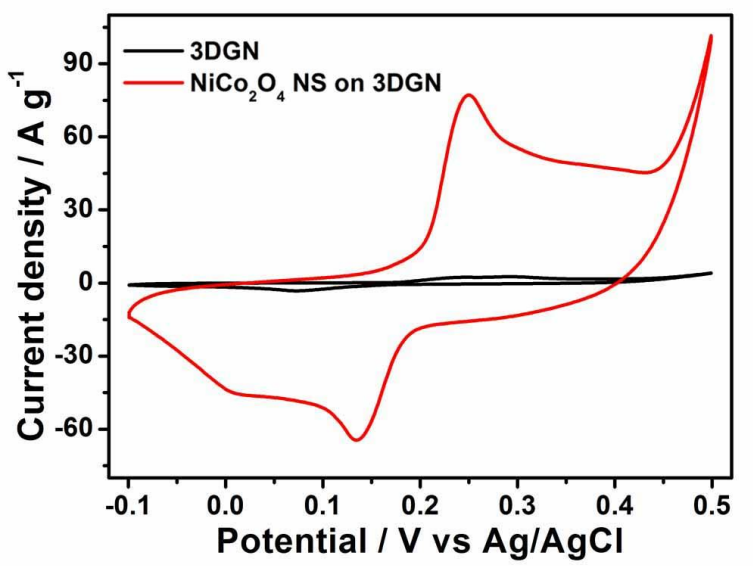

Figure S10. The cyclic voltammograms (CVs) of pure 3DGN and $NiCo_2O_4$ NS/3DGN at a scan rateof 20 mV s^{-1}.The potential range of CV test is from -0.1 to 0.5 V (vs. standard Ag/AgCl electrode).

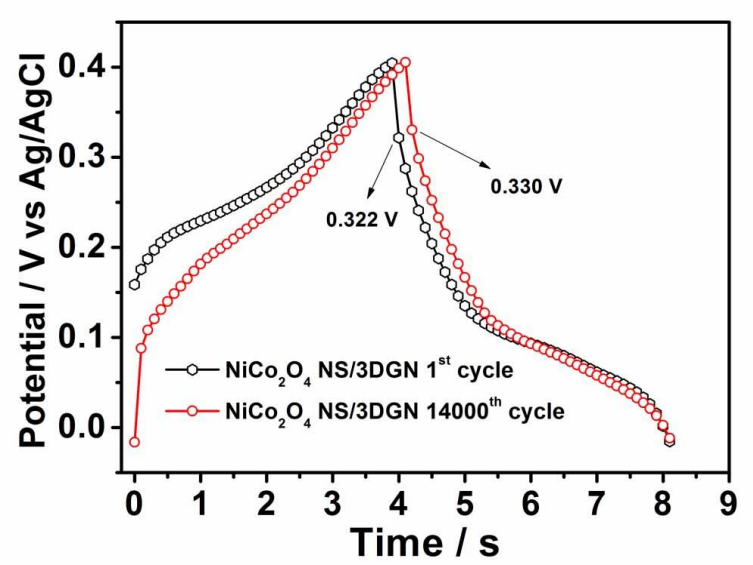

Figure S11. The first and last charge/discharge curves of $NiCo_2O_4$ NS/3DGN electrode at the current density of 100 A g^{-1}. The potential range is from 0 to 0.4 V (vs. standard Ag/AgCl electrode).

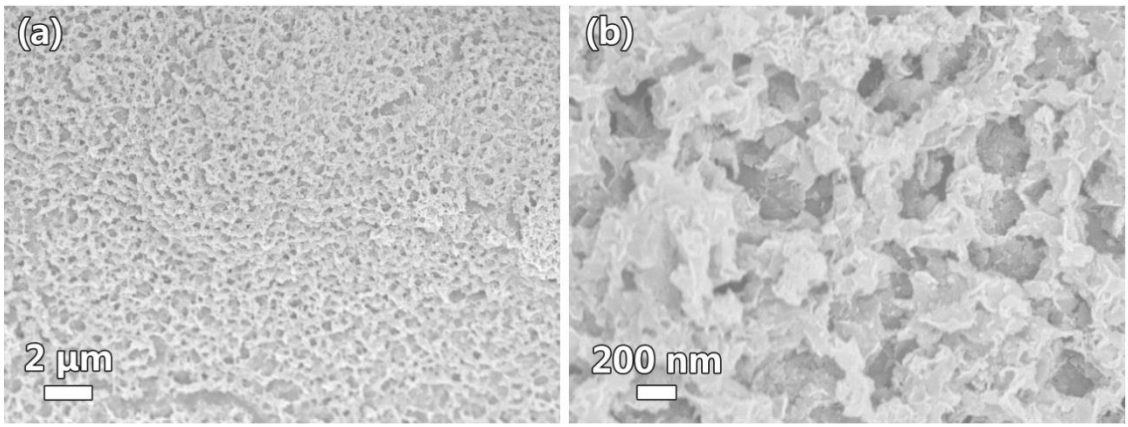

Figure S12. SEM images of $NiCo_2O_4$ NS/3DGN electrode after 14000 cycles at 100 A g^{-1}.

Table S1. Comparison of electrochemical properties of $NiCo_2O_4$-based materials, metal oxides, metal hydroxides and their hybrid composites.

Electrode material	Capacitance	Capacitance retention	Ref.
Thin 2D $NiCo_2O_4$ nanosheet-coated 3D graphene network	2173 F g^{-1} (6 A g^{-1}) 1941 F g^{-1} (20 A g^{-1}) 954 F g^{-1} (200 A g^{-1})	100 % after 2800 cycles (20 A g^{-1}) 94 % after 14000 cycles (100 A g^{-1})	This work
$NiCo_2O_4$ nanosheets on Ni foam	1743 F g^{-1} (7 A g^{-1}) 1065 F g^{-1} (21 A g^{-1})	83 % after 3000 cycles (21 A g^{-1})	19
$NiCo_2O_4$ nanowires on carbon textiles	1283 F g^{-1} (1 A g^{-1}) 1010 F g^{-1} (20 A g^{-1})	~100 % after 5000 cycles (8 A g^{-1})	8
$NiCo_2O_4$ nanosheets on Ni foam	2010 F g^{-1} (2 A g^{-1}) 1450 F g^{-1} (20 A g^{-1})	94 % after 2400 cycles (2 A g^{-1})	6
$NiCo_2O_4$ nanosheets@ halloysite nanotubes	1887 F g^{-1} (6 A g^{-1}) 1500 F g^{-1} (30 A g^{-1})	95 % after 8600 cycles (10 A g^{-1})	20
$NiCo_2O_4$ nanowire cluster array on Ni foam	2131 F g^{-1} (10 A g^{-1}) 1069 F g^{-1} (100 A g^{-1})	94 % after 10200 cycles (10 A g^{-1})	21
Carbon-CoO-NiO-$NiCo_2O_4$ hybrid	2602 F g^{-1} (2 mA cm^{-2})	Rising trend after 7000 cycles (50 mA cm^{-2})	22
$NiCo_2O_4$ noneedles on Ni foam	1119 F g^{-1} (5.56 mA cm^{-2})	89 % after 2000 cycles (5.56 mA cm^{-2})	23
$NiCo_2O_4$/carbon aerogel composite	1700 F g^{-1} (25 mV s^{-1}) 800 F g^{-1} (500mV s^{-1})	98 % after 2000 cycles (500 mV s^{-1})	24
Porous $NiCo_2O_4$ Nanotubes	1648 F g^{-1} (1 A g^{-1}) 1274 F g^{-1} (25 A g^{-1})	94 % after 3000 cycles (10 A g^{-1})	25
Au nanoparticles decorated $NiCo_2O_4$	1390 F g^{-1} (5 A g^{-1}) 530 F g^{-1} (100 A g^{-1})	85 % after 10000 cycles (10 A g^{-1})	26
Nickel-Cobalt Hydroxide/$NiCo_2O_4$	~1.64 F/cm^2 (2 mA cm^{-2})	81 % after 2000 cycles (2 mA cm^{-2})	27
$NiCo_2O_4$ nanosheets on carbon nanofibers	1002 F g^{-1} (1 A g^{-1}) 520 F g^{-1} (20 A g^{-1})	93 % after 2400 cycles (5 A g^{-1})	28
Hierarchical mesoporous $NiCo_2O_4$	1619 F g^{-1} (2 A g^{-1}) 571 F g^{-1} (10 A g^{-1})	Very slight decrease after 1000 cycles (6 A g^{-1})	5
$NiCo_2O_4$@MnO_2 nanowires on Ni foam	~3.31 F/cm^2 (2 mA cm^{-2})	88 % after 2000 cycles	29
$NiCo_2O_4$ nanowires	1284 F g^{-1} (2 A g^{-1}) 986 F g^{-1} (20 A g^{-1})	98 % after 3000 cycles (50 mV s^{-1})	30
$NiCo_2O_4$@$NiCo_2O_4$ core-shell nanoarrays	1925 F g^{-1} (0.5 A g^{-1}) 1470 F g^{-1} (20 A g^{-1})	90 % after 3500 cycles (5 A g^{-1})	31
$NiCo_2O_4$@$Co_xNi_{1-x}(OH)_2$ nanosheet arrays	1045 F g^{-1} (1 A g^{-1})	83 % after 3000 cycles (50 mV s^{-1})	32
$NiCo_2O_4$@graphene nanoarchitectures	778 F g^{-1} (1 A g^{-1}) 374 F g^{-1} (80 A g^{-1})	90 % after 10000 cycles (10 A g^{-1})	33
CNT/$NiCo_2O_4$ core/shell structure	695 F g^{-1} (1 A g^{-1}) 576 F g^{-1} (20 A g^{-1})	91 % after 1500 cycles (4 A g^{-1})	34
CNT@ $NiCo_2O_4$ core–shell hybrid	1038 F g^{-1} (0.5 A g^{-1}) 667 F g^{-1} (10 A g^{-1})	100 % after 1000 cycles (2 A g^{-1})	35

$NiCo_2O_4$@$CoMoO_4$ on Ni foam	15 F g^{-1} (2 A g^{-1}) (10 mA cm^{-2})	74 % after 1000 cycles (5 A g^{-1}) (60 mA cm^{-2})	36
$NiCo_2O_4$ nanosheet on carbon fabric	2658 F g^{-1} (2 A g^{-1}) 1866 F g^{-1} (20 A g^{-1})	80 % after 3000 cycles 10 A g^{-1})	37
$NiCo_2O_4$ microsphere	1006 F g^{-1} (1 A g^{-1})	93 % after 1000 cycles (8 A g^{-1})	13
$NiCo_2O_4$ hierarchitectures	1191 F g^{-1} (1 A g^{-1}) 755 F g^{-1} (10 A g^{-1})	78 % after 1200 cycles (1 A g^{-1})	15
Hollow $NiCo_2O_4$ sub-microspheres	678 F g^{-1} (1 A g^{-1}) 540 F g^{-1} (10 A g^{-1})	87 % after 3500 cycles (10 A g^{-1})	38
3D Graphene-CoO nanorods	980 F g^{-1} (1 A g^{-1}) 600 F g^{-1} (20 A g^{-1})	103 % after 10000 cycles (5 A g^{-1})	12
Co_3O_4/rGO/CNTs hybrid paper	378 F g^{-1} (2 A g^{-1}) 297 F g^{-1} (8 A g^{-1})	96 % after 3000 cycles (2 A g^{-1})	39
Co_3O_4/carbon nanofibers	552 F g^{-1} (1 A g^{-1}) 403 F g^{-1} (12 A g^{-1})	99 % after 2000 cycles (4 A g^{-1})	40
Co_3O_4 nanosheets on Ni foam	2735 F g^{-1} (2 A g^{-1}) 1471 F g^{-1} (10 A g^{-1})	~99 % after 3000 cycles (8 A g^{-1})	41
Nanostructured α-$Co(OH)_2$	881 F g^{-1} (1 A g^{-1}) 772 F g^{-1} (10 A g^{-1})	91 % after 2000 cycles	42
Porous β‑$Co(OH)_2$ architecture	416 F g^{-1} (1 A g^{-1}) 320 F g^{-1} (5 A g^{-1})	93 % after 500 cycles (1 A g^{-1})	43
NiO/Cnanofibers	288 F g^{-1} (0.3 A g^{-1})	89 % after 3000 cycles (0.3 A g^{-1})	44
Co/NiO core/shell nanowire arrays	956 F g^{-1} (2 A g^{-1}) 737 F g^{-1} (40 A g^{-1})	98 % after 6000 cycles (2 A g^{-1})	45
Au–NiO hierarchical structures	765 F g^{-1} (2 A g^{-1}) 619 F g^{-1} (20 A g^{-1})	90 % after 2000 cycles (4 A g^{-1})	46
Porous NiO nanocomposite	430 F g^{-1} (0.2 A g^{-1}) 261 F g^{-1} (2 A g^{-1})	86 % after 2000 cycles (1 A g^{-1})	47
Cu@$Ni(OH)_2$ nanobelts	2426 F g^{-1} (10 A g^{-1}) 1965 F g^{-1} (100 A g^{-1})	91 % after 1000 cycles (30 A g^{-1})	48
Nanoporous $Ni(OH)_2$ 3D Graphite Foam	166 F g^{-1} (0.5 A g^{-1}) 111 F g^{-1} (10 A g^{-1})	65 % after 1000 cycles (10 A g^{-1})	10
$Ni(OH)_2$@$Co(OH)_2$	369 F g^{-1} (1 A g^{-1})	96 % after 2500 cycles (1 A g^{-1})	49
RuO_2/graphene sheet composites	570 F g^{-1} (1 mV s^{-1}) 268 F g^{-1} (50 mV s^{-1})	98 % after 1000 cycles (1 A g^{-1})	50
Graphene/MnO_2	256 F g^{-1} (0.5 A g^{-1})	74 % after 1000 cycles (0.5 A g^{-1})	51
Co_3O_4@MnO_2 Core/Shell arrays	480 F g^{-1} (2.67 A g^{-1}) 267 F g^{-1} (29.8 A g^{-1})	97 % after 5000 cycles (11.25 mA cm^{-2})	52
Highly ordered MnO_2 nanopillars	603 F g^{-1} (5 mV s^{-1})	93 % after 5000 cycles (1000 mV s^{-1})	53
Zn_2SnO_4/MnO_2core/Shell nanocable-carbon	642 F g^{-1} (1 A g^{-1}) 414 F g^{-1} (40 A g^{-1})	99 % after 1000 cycles (10 A g^{-1})	54
MnO_2/graphene hybrid	254 F g^{-1} (0.5 A g^{-1}) 208 F g^{-1} (10 A g^{-1})	92 % after 7000 cycles	55
Graphene/MnO_2 nanostructured	~380 F g^{-1} (0.1 mA cm^{-2})	95 % after 3000 cycles (1 mA cm^{-2})	56
$ZnCo_2O_4$ nanowire arrays on Ni foam	1625 F g^{-1} (5 A g^{-1}) 962 F g^{-1} (80 A g^{-1})	94 % after 5000 cycles (20 A g^{-1})	57
$ZnCo_2O_4$ nanosheet arrays on Ni foam	2468 F g^{-1} (5 A g^{-1}) 1482 F g^{-1} (100 A g^{-1})	96 % after 1500 cycles (30 A g^{-1})	58

$NiMoO_4$ nanospheres	974 F g^{-1} (1 A g^{-1}) 821 F g^{-1} (10 A g^{-1})	74 % after 2000 cycles (5 A g^{-1})	59
$NiMoO_4$ nanosheets on Ni foam	3205 F g^{-1} (5mA cm^{-2}) 1881 F g^{-1} (30 mA cm^{-2})	87 % after 2000 cycles (15mA cm^{-2})	60
Co_3O_4@$NiMoO_4$ nanowires on Ni foam	1230 F g^{-1} (10 mA cm^{-2}) 970 F g^{-1} (80 mA cm^{-2})	77 % after 3000 cycles (50 mA cm^{-2})	61
$CoMoO_4$/$NiMoO_4$•xH_2O bundles	1039 F g^{-1} (2.5 mA cm^{-2}) 750 F g^{-1} (100 mA cm^{-2})	72 % after 1000 cycles (25 A g^{-1})	62
$CoMoO_4$ nanoplate arrays on Ni foam	1558 F g^{-1} (64 A g^{-1})	80 % after 4000 cycles (12 mA cm^{-2})	63

References

1. X. Cao, Y. Shi, W. Shi, X. Rui, Q. Yan, J. Kong and H. Zhang, *Small*, 2013,**9**, 3433.
2. X. Cao, Y. Shi, W. Shi, G. Lu, X. Huang, Q. Yan, Q. Zhang and H. Zhang, *Small*, 2011, **7**, 3163.
3. X. Cao, B. Zheng, X. Rui, W. Shi, Q. Yan and H. Zhang, *Angew. Chem. Int. Ed.*, 2014, **53**, 1404.
4. L. Mai, F. Yang, Y. Zhao, X. Xu, L. Xu and Y. Luo, *Nat. Commun.*, 2011, **2**, 381.
5. Y. Zhang, M. Ma, J. Yang, H. Su, W. Huang and X. Dong, *Nanoscale*, 2014, **6**, 4308.
6. C. Yuan, J. Li, L. Hou, X. Zhang, L. Shen and X. Lou, *Adv. Funct. Mater.*, 2012, **22**, 4592.
7. Z. Liu, Q. Xu, J. Wang, N. Li, S. Guo, Y. Su, H. Wang, J. Zhang and S. Chen, *Int. J. Hydrogen Energ.*, 2013, **38**, 6657.
8. L. Shen, Q. Che, H. Li and X. Zhang, *Adv. Funct. Mater.*, 2014, **24**, 2630.
9. X. Dong, H. Xu, X. Wang, Y. Huang, M. Chan-Park, H. Zhang, L. Wang, W. Huang and P. Chen, *ACS Nano*, 2012, **6**, 3206.
10. J. Ji, L. Zhang, H. Ji, Y. Li, X. Zhao, X. Bai, X. Fan, F. Zhang and R. Ruoff, *ACS Nano*,2013, **7**, 6237.
11. W. Zhou, X. Cao, Z. Zeng, W. Shi, Y. Zhu, Q. Yan, H. Liu, J. Wang and H. Zhang, *Energy Environ. Sci.*, 2013, **6**, 2216.
12. Y. G. Zhu, Y. Wang, Y. Shi, Z. X. Huang, L. Fu and H. Y. Yang, *Adv. Energy Mater.*, 2014, **4**, 1301788.
13. Y. Lei, J. Li, Y. Wang, L. Gu, Y. Chang, H. Yuan and D. Xiao, *ACS Appl. Mater. Inter.*, 2014, **6**, 1773.
14. R. Ding, L. Qi, M. Jia and H. Wang, *Nanoscale*, 2014, **6**, 1369.

15. C. An, Y. Wang, Y. Huang, Y. Xu, C. Xu, L. Jiao and H. Yuan, *CrystEngComm*, 2014, **16**, 385.
16. X. Lu, D. Wu, R. Li, Q. Li, S. Ye, Y. Tong and G. Li, *J. Mater. Chem. A*, 2014, **2**, 4706
17. C. Yuan, J. Li, L. Hou, L. Yang, L. Shen and X. Zhang, *J. Mater. Chem.*, 2012, **22**, 16084.
18. J. Li, S. Xiong, Y. Liu, Z. Ju and Y. Qian, *ACS Appl. Mater. Inter.*, 2013, **5**, 981.
19. G. Zhang and X. W. Lou, *Adv. Mater.*, 2013, **25**, 976.
20. J. Liang, Z. Fan, S. Chen, S. Ding and G. Yang, *Chem. Mater.*, 2014, **26**, 4354.
21. Y. Chen, B. Qu, L. Hu, Z. Xu, Q. Li and T. Wang, *Nanoscale*, 2013, **5**, 9812.
22. H. Wang, J. Guo, C. Qing, D. Sun, B. Wang and Y. Tang, *Chem. Commun.*, 2014, **50**, 8697.
23. G.Zhang, H. Wu, H. Hoster, M. Chan-Park and X. Lou, *Energy Environ. Sci.*,2012, **5**, 9453.
24. H. Chien, W. Cheng, Y. Wang and S. Lu, *Adv. Funct. Mater.*,2012, **22**, 5038.
25. L. Li, S. Peng, Y. Cheah, P. Teh, J. Wang, G. Wee, Y. Ko, C. Wong and M. Srinivasan, *Chem. Eur. J.*,2013, **19**, 5892.
26. J. Zhu, Z. Xu and B. Lu, *Nano Energy*, 2014, **7**, 114.
27. L. Huang, D. Chen, Y. Ding, S. Feng, Z. L. Wang and M. Liu, *Nano Lett.*, 2013, **13**, 3135.
28. G. Zhang and X. Lou, *Sci. Rep.*, 2013, **3**, 1470.
29. L. Yu, G. Zhang, C. Yuan and X. Lou, *Chem. Commun.*, 2013, **4**9, 137.
30. R. Zou, K. Xu, T. Wang, G. He, Q. Liu, X. Liu, Z. Zhang and J. Hu, *J. Mater. Chem. A*, 2013, **1**, 8560.
31. W. Zhou, D. Kong, X. Jia, C. Ding, C. Cheng and G. Wen, *J. Mater. Chem. A*, 2014, **2**, 6310.
32. K. Xu, R. Zou, W. Li, Q. Liu, X. Liu, L. An and J. Hu, *J. Mater. Chem. A*,2014, **2**, 10090.
33. Y. Wei, S. Chen, D. Su, B. Sun, J. Zhu and G. Wang, *J. Mater. Chem. A*, 2014, **2**, 8103.
34. W. Liu, C. Lu, K. Liang and B. Tay, *J. Mater. Chem. A*, 2014, **2**, 5100.
35. F. Cai, Y. Kang, H. Chen, M. Chen and Q. Li, *J. Mater. Chem. A*, 2014, **2**, 11509.
36. D. Cai, B. Liu, D. Wang, L. Wang, Y. Liu, H. Li, Y. Wang, Q. Li and T. Wang, *J. Mater. Chem. A*, 2014, **2**, 4954.

37. J. Du, G. Zhou, H. Zhang, C. Cheng, J. Ma, W. Wei, L. Chen and T. Wang, *ACS Appl. Mater. Inter.*,2013, **5**, 7405.
38. C. Yuan, J. Li, L. Hou, J. Lin, G. Pang, L. Zhang, L. Lian and X. Zhang, *RSC Adv.*, 2013, **3**, 18573.
39. C. Yuan, L. Yang, L. Hou, J. Li, Y. Sun, X. Zhang, L. Shen, X. Lu, S. Xiong and X. W. D. Lou, *Adv. Funct. Mater.*, 2012, **22**, 2560.
40. F. Zhang, C. Yuan, J. Zhu, J. Wang, X. Zhang and X. W. D. Lou, *Adv. Funct. Mater.*, 2013, **23**, 3909.
41. C. Yuan, L. Yang, L. Hou, L. Shen, X. Zhang and X. Lou, *Energy Environ. Sci.*, 2012, **5**, 7883.
42. V. Gupta, T. Kusahara, H. Toyama, S. Gupta and N. Miura, *Electrochem. Commun.*, 2007, **9**, 2315.
43. C. Mondal, M. Ganguly, P. K. Manna, S. M. Yusuf and T. Pal, *Langmuir*, 2013, **29**, 9179.
44. D. H. Shin, J. S. Lee, J. Jun and J. Jang, *J. Mater. Chem. A*, 2014, **2**, 3364.
45. G. X. Pan, X. H. Xia, F. Cao, P. S. Tang and H. F. Chen, *Electrochem. Commun.*,2013, **34**, 146.
46. B. Qu, L. Hu, Y. Chen, C. Li, Q. Li, Y. Wang, W. Wei, L. Chen and T. Wang, *J. Mater. Chem. A*,2013, **1**, 7023.
47. Y. Jiang, D. Chen, J. Song, Z. Jiao, Q. Ma, H. Zhang, L. Cheng, B. Zhao and Y. Chu, *Electrochim. Acta*, 2013, **91**, 173.
48. I. Chang, T. Chen, M. Yang, H. Chiu and C. Lee, *J. Mater. Chem. A*, 2014, **2**, 10370.
49. D. Zhou, X. Su, M. Boese, R. Wang and H. Zhang, *Nano Energy*, 2014, **5**, 52.
50. Z. Wu, D. Wang, W. Ren, J. Zhao, G. Zhou, F. Li and H. Cheng, *Adv. Funct. Mater.*, 2010, **20**, 3595.
51. Z. Li, Y. Mi, X. Liu, S. Liu, S. Yang and J. Wang, *J. Mater. Chem.*, 2011, **21**, 14706.
52. J. Liu, J. Jiang, C. Cheng, H. Li, J. Zhang, H. Gong and H. J. Fan, *Adv. Mater.*, 2011, **23**, 2076.
53. Z. Yu, B. Duong, D. Abbitt and J. Thomas, *Adv. Mater.*, 2013, **25**, 3302.
54. L. Bao, J. Zang and X. Li, *Nano Lett.*, 2011, **11**, 1215.
55. L. Peng, X. Peng, B. Liu, C. Wu, Y. Xie and G. Yu, *Nano Lett.*, 2013, **13**, 2151.
56. G. Yu, L. Hu, N. Liu, H. Wang, M. Vosgueritchian, Y. Yang, Y. Cui and Z. Bao, *Nano Lett.*, 2011, **11**, 4438.

57. S. Wang, J. Pu, Y. Tong, Y. Cheng, Y. Gao and Z. Wang, *J. Mater. Chem. A*, 2014, **2**, 5434.
58. F. Bao, X. Wang, X. Zhao, Y. Wang, Y. Ji, H. Zhang and X. Liu, *RSC Adv.*, 2014, **4**, 2393.
59. D. Cai, D. Wang, B. Liu, Y. Wang, Y. Liu, L. Wang, H. Li, H. Huang, Q. Li and T. Wang, *ACS Appl. Mater. Inter.*, 2013, **5**, 12905.
60. D. Cai, B. Liu, D. Wang, Y. Liu, L. Wang, H. Li, Y. Wang, C. Wang, Q. Li and T. Wang, *Electrochim. Acta*, 2014, **125**, 294.
61. D. Cai, D. Wang, B. Liu, L. Wang, Y. Liu, H. Li, Y. Wang, Q. Li and T. Wang, *ACS Appl. Mater. Inter.*, 2014, **6**, 5050.
62. M. Liu, L. Kong, C. Lu, X. Ma, X. Li, Y. Luo and L. Kang, *J. Mater. Chem. A*,2013, **1**, 1380.
63. D. Guo, H. Zhang, X. Yu, M. Zhang, P. Zhang, Q. Li and T. Wang, *J. Mater. Chem. A*,2013, **1**, 7247.